

## Evaluation of Mechanical Properties and Microstructure of Sol–Gel Derived Zirconia-Hydroxiapatite Nanocomposite Coatings

Moluk Aivazi<sup>1\*</sup>, Mohammadhossein Fathi<sup>1,2</sup>, Farahnaz Nejatidanesh<sup>2</sup>, Vajihesadat Mortazavi<sup>3</sup> and Batoul HashemiBani<sup>4</sup>

<sup>1</sup>Biomaterials Research Group, Department of Materials Engineering, Isfahan University of Technology, Isfahan, Iran

<sup>2</sup>Dental Materials Research Center, School of Dentistry, Isfahan University of Medical Sciences, Isfahan, Iran

<sup>3</sup>Torabinejad Dental Research Center, Department of Operative Dentistry, School of Dentistry, Isfahan University of Medical Sciences, Isfahan, Iran

<sup>4</sup>Department of Anatomical Sciences and Molecular Biology, School of Medicine, Isfahan University of Medical Sciences, Isfahan, Iran

\*Corresponding Author: Moluk Aivazi, Biomaterials Research Group, Department of Materials Engineering, Isfahan University of Technology, Isfahan, Iran.

Received: October 12, 2016; Published: December 26, 2016

### Abstract

One way to control zirconia degradation process at low temperature is alumina addition to zirconia matrix. Another way is creating a coat with minimal cracks and pits on zirconia substrate for endosseous dental implant application. Deposition of a yttrium stabilized tetragonal zirconia polycrystal– hydroxyapatite (3Y-TZP-HA) coating may limit water penetration into the zirconia substrate. The aim of this study was surface treatment of alumina (20% vol)- yttrium - stabilized tetragonal zirconia (A-3Y-TZP20) nano-composite using the 3Y-TZP-HA coating with minimal cracks and pits. Toward this purpose, the 3Y-TZP (10% wt)-HA coating was deposited onto A-3Y-TZP20 nano-composite substrate by utilizing the sol–gel method. The morphology, phase composition and dissolution behavior of the coatings were characterized by scanning electron microscopy (SEM), X-ray diffraction (XRD), and transmission electron microscopy (TEM), techniques. Also, the mechanical properties of the coatings were evaluated. Comparison of HA and HA-3Y-TZP in terms of young's modulus and hardness means showed that p-values ( $p \leq 0.05$ ) were significant. Also, a lower dissolution rate of calcium and phosphorus ions was obtained for the 3Y-TZP-HA coat, with respect to HA, mainly due to the difference in the chemical composition of these coatings. It was concluded that the 3Y-TZP- HA nano-composite coating with minimal cracks and pits could be introduced as a promising way for the further control of the low temperature degradation process.

**Keywords:** 3Y-TZP-HA Coat; A-3Y-TZP20 Nano-Composite; Sol-Gel; Mechanical Properties

### Introduction

Titanium and its alloys are usually used as intraosseous dental implants [1-4]. The first interaction between the implant and the host tissue occurs at the interface with an area almost equal to that of a water molecule. In the case of titanium implants, almost 1600 ppm of titanium ions appears in the haversian channel while the natural level of titanium should not exceed 50 ppm in human's body, but its level could reach 300 ppm in the adjacent tissues [5]. Numerous studies have shown that the tissue reaction causing titanium release varies from mild to severe [6]. Therefore, bioceramic materials have been introduced as alternatives to titanium implants. In this respect, the 3Y-TZP ceramics are of great interest due to mechanical characteristics similar to those of metals and some white color like that of teeth [7]. The surface characteristics of the implant affect the bone responses. The bone-implant interactions can be controlled by changing

the morphological, physical and biochemical properties of biomaterials. These changes can be made through surface roughening, blasting, etching and surface energy modification [5]. The surface of zirconia implants has been modified by different approaches to improve osseointegration (acid etching, sandblasting, laser treatment, or a combination of these methods) and it has been evaluated by torque removal or bone implant contact measurement [8-12]. But zirconia is prone to the low temperature degradation process when it is used in wet environments or oral spaces [7]. One way to reduce low temperature degradation is alumina addition. Another way is creating a free crack and pit coating on zirconia to reduce water penetration into the substrate layer. Also, HA deposition as a surface modification method has been widely studied to improve the osseointegration of dental implants [13]. Biocompatibility, bioactivity and osteo-conductivity of hydroxyapatite are well-known in biomaterial applications. But the low mechanical strength and fracture toughness of HA are the main drawbacks limiting its performance for load-bearing applications [13-14]. It is well-established that sand blasting and surface micro-roughening processes improve the interfacial bonding between coating and ceramic substrate by applying residual compressive stress, leading to the higher surface area and greater physical and chemical activity [15]. Besides, an improved bone response has been reported for the surface with the average roughness of 1 - 1.5 micrometers, as compared to the implants with a smooth surface [5]. Also, sand blasting decreases the stress concentration and bone resorption by increasing the surface area and mechanical interlocking at the bone-coating interface [15]. Several methods are used for the deposition of HA coatings onto the implants, among which plasma spraying is the only commercial method. Sol-gel process, as a simple and inexpensive method, provides several advantages over plasma spraying, such as higher purity and homogeneity, lower process temperature, and more controllable coating thickness [14]. The mechanical properties of HA can be improved by several methods including, but not limited to, the synthesis of composite materials containing HA and a second phase such as zirconia, and the deposition of HA coating onto strong biomaterials like zirconia or titanium alloy. Vasconcelos, *et al.* [16] studied the mechanical properties of 3Y-TZP-HA composite developed by the modified sol-gel method, revealing an increase in hardness and fracture toughness by adding 10%wt of zirconia to hydroxiapatite. The investigations by Evis [17] in the case of HA-ZrO<sub>2</sub> (10-40 wt.%) disks showed that the maximum osteoblast adhesion was achieved for the composite disks with 10 wt.% ZrO<sub>2</sub>. In these circumstances, the biocompatibility and bioactivity are provided by apatite phase and the mechanical properties, especially fracture toughness stemming from ZrO<sub>2</sub> (10% wt) phase. This is because zirconia ceramic have the highest fracture toughness among all bioceramic materials. Therefore, this study was aimed at evaluating the mechanical properties and the dissolution rate of 3Y-TZP(10% wt) -HA nano-composite coating deposited on the alumina (20%vol)-yttrium-stabilized tetragonal zirconia (A-3Y-TZP20) substrate for endosseous dental implant applications using the sol-gel method.

## Materials and Methods

### Deposition of 3Y-TZP-HA coating

Alumina (20% vol) - yttrium stabilized tetragonal zirconia polycrystal nano-composite disks with the dimension of  $\emptyset 12 \times 1.2$  mm were used. Nano-sized Al<sub>2</sub>O<sub>3</sub> ( $\alpha$ -Al<sub>2</sub>O<sub>3</sub> purity > 99/99%, average particle size of 13 nm, sigma aldrich, U.S.A) and Y-TZP (Y-TZP, Particle size < 100 nm, sigma aldrich, U.S.A) powders were used as the starting materials. After sieving, the powders were uniaxially pressed into disks with the dimension of  $\emptyset 12 \times 1.2$  mm under a pressure of 150 MPa [19]. An A-3Y-TZP nano-composite containing 20 vol.% alumina was sintered at 1270°C for 170 min in air and used as the substrate. The A-YTZP 20 nanocomposite disks were obtained in the biomaterial laboratory of Isfahan University of Technology. The sintered A-3Y-TZP20, with the dimensions of  $\emptyset 12 \times 1.2$  mm and the average grain size of < 400 nm, was almost fully dense with the theoretical density of above 96%, as measured by the kern system (ALS series). The A-3Y-TZP20 substrates were sand blasted using alumina particles (with the size of ~60  $\mu$ m). Surface roughness was measured by mitutoyo system. For the deposition of 3Y-TZP-HA nano-composite coat on A-3Y-TZP20 nano-composite substrate, the precursors of calcium nitrate [Ca(NO<sub>3</sub>)<sub>2</sub>·4H<sub>2</sub>O, Merck, Germany] and phosphorus pentoxide [P<sub>2</sub>O<sub>5</sub>, Merck, Germany] were used as the starting materials [18]. Toward this purpose, stoichiometric amounts of the precursors were separately dissolved in ethanol under stirring condition for 20 min. Then, the Ca-containing solution was slowly added to a P-containing solution and stirred for 1h. To prevent crack formation in the coating, a certain amount of oxalic acid (2% weight solution) was added and the solution was stirred for another 1h. Finally, a solution containing

10 wt.%3Y-TZP (with the particle size of < 100 nm, Sigma-Aldrich, USA) was incorporated into the former solution and stirred for 4h to prepare the 3Y-TZP-HA sol. The [Ca]/[P] ratio of the 3Y-TZP-HA sol was adjusted to 1.67. For comparison, HA sol without 3Y-TZP was also prepared by the same procedure, except for the last step. Prior to coating deposition, the substrates were ultrasonically cleaned by immersing in acetone, alcohol and distilled water for 20 min, after which the substrates were dried in the oven at 120°C for 24h. The 3Y-TZP-HA coats were deposited onto A-3Y-TZP20 substrates by a dip coating process with a speed of 30 mm per min. The obtained coats were aged at room temperature for 24h, dried in the oven at 80°C for another 24 h, and finally, heat treated at 600°C for 1h. The heating and cooling rates were adjusted to 1°C/min.

### Microstructural and Mechanical characterizations

Phase composition of the coatings, after heat treatment, was determined by x-ray diffraction (XRD) (Philips diffractometer, 40 kV, Cu K $\alpha$  radiation:  $\lambda = 0.15418$  nm) in the  $2\theta$  range of 20-80°, with the step size of 5°/sec. The surface morphology of the coatings was examined by scanning electron microscopy (SEM) (Phillips, XL30). Young's modulus, hardness and fracture toughness of the coatings were measured by nanoindentation testing (NHT compact platform, NHT-epx, CSM) over a load range of 30 mN and a penetration depth equal to 0.1 of coating thickness [20]. Fracture toughness (KIC) of the coatings was obtained by measuring the accurate size of the cracks formed during nanoindentation [21]. Toward this purpose, the indented surface was examined by an in-situ atomic force microscopy (AFM) to capture the features of cracks. Then, the fracture toughness of the samples was calculated using the following equation

$$KIC = \alpha [E/H]^{1/2} [P/c^{3/2}]$$

where KIC is indentation fracture toughness,  $\alpha$  is a constant related to the tip geometry, E is young's modulus determined through nanoindentation and the poisson's ratio of the material [22], H is hardness, P is the maximum load, and c is the average crack length from the indenter corner to the end of crack [23].

### Evaluation of the dissolution behavior of HA and HA- ZrO<sub>2</sub> coat

To evaluate the dissolution behavior, the 3Y-TZP-HA and HA coatings deposited on A-3Y-TZP20 nano-composite and calcined at 600°C were immersed in a physiological saline solution (0.9% NaCl) and aged in water bath at 37°C, by following the Kim's studies [24]. At predetermined incubation periods, the sample was removed and the concentration of Ca and P ions was determined using inductively coupled plasma-atomic emission spectroscopy(ICP-AES) ICPS-100IV, Shimadzu). For comparison, a pure HA coating was also examined in terms of dissolution behavior.

## Results

### Roughness measurement

Sand blasting was used to modify the implant surface using alumina particles. The surface roughness parameters of sand blasted substrates were measured to be: Ra: 2.836  $\mu$ m, Rq: 3.671  $\mu$ m, and Rz: 17.256  $\mu$ m.

### XRD analysis

Figure 1 shows the XRD patterns of HA and 3Y-TZP-HA coatings after heat treatment. In the XRD –patterns of coatings after heat treatment, without applying on the substrate (see Figure1), only the calcium oxide phase was present in the HA coat. The other peaks in the XRD-patterns of 3Y-TZP-HA(B) and HA(A) coatings are shown in Figure 1.

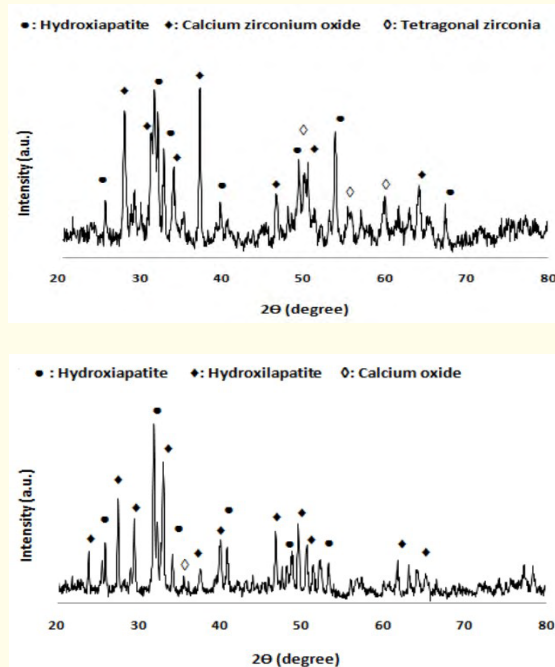


**Figure 1:** XRD patterns of (A) HA and (B) 3Y-TZP-HA coating after heat treatment at 600°C for 1h without applying on A-3Y-TZP20 substrate.

**SEM observations**

To achieve free crack and pit coating, the morphology of HA(A) and 3Y-TZP-HA(B) coatings heat treated at 600, 700 and 900°C with aging times of 24, 18 and 12h, respectively, were evaluated by SEM. As shown in Figure 2, the existence of cracks and pits was clearly observed for the coatings heat treated at 900°C, while by reducing the temperature to 700°C and increasing the aging time to 18h, the minimal pits and cracks took place. Further decreasing the temperature to 600°C and increasing the aging time to 24h resulted in the formation of a free-crack 3Y-TZP-HA and HA coatings on A-3Y-TZP20 substrate (Figure 2). According to TEM image shown in Figure 3, the presence of the nano-sized 3Y-TZP-HA coating with the grain size of < 50 nm was evident in the 3Y-TZP-HA nano-composite coat.

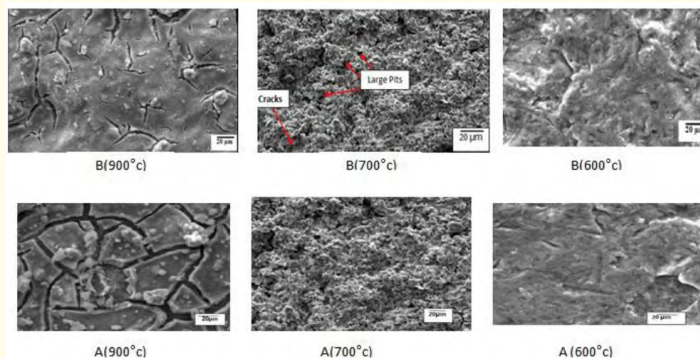


**Figure 2:** SEM images from HA (A) and 3Y-TZP-HA(B) coating after heat treatment at 900°C, 700°C and 600°C with the aging time 12h, 18h and 24h, respectively.

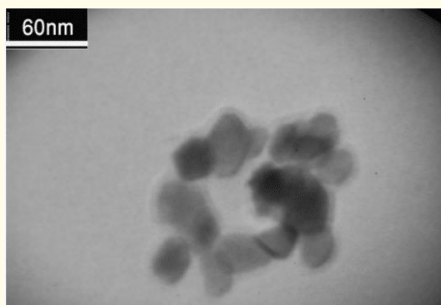


Figure 3: TEM image from the optimized 3Y-TZP -HA coating.

### Mechanical properties

Comparison of young’s modulus and hardness means in HA and HA-3Y-TZP groups showed that p-values were significant (0.04 for young’s modulus and 0.00 for hardness). In other words, the HA-3Y-TZP nano-composite coat showed higher young’s modulus and hardness (Table 1). Figure 4 shows the effect of nanoindenter on 3Y-TZP-HA nanocomposite coating. Also, Figure 5 presents the variation of hardness and young’s modulus of coatings versus zirconia content. It could be observed that the young’s modulus and hardness of the coatings were increased in the ranges of 149.6-214 GPa and 5.981-12.34 GPa, by increasing the zirconia content from 0 to 10wt%, thereby indicating superior mechanical properties of 3Y-TZP-HA coating, in comparison to those of HA coating. This improvement in mechanical behavior could be attributed to the presence of ZrO<sub>2</sub> phase combined with the formation of nano-structured 3Y-TZP-HA coat. As shown in Figure 6, the fracture toughness of coatings was increased in the range of 1.48 - 3.53 MPa.m<sup>1/2</sup> with increasing the zirconia content from 0 to 10 wt.%.

Variable	Young’s modulus (G Pa)	Hardness (Kg/mm <sup>2</sup> )
<b>Group</b>		
HA coat (mean ± S.D)	149 ± 23.8	609.28 ± 8.78
HA-3Y-TZP coat (mean ± S.D)	214.02 ± 5.92	1258.2 ± 14.2
P* ≤ 0.05	0.04	0.00

Table 1: Statistical results from the comparison of the young’s modulus and hardness means between HA and HA-3Y-TZP coats.

P\* - value is significant at level of ≤ 0.0 5

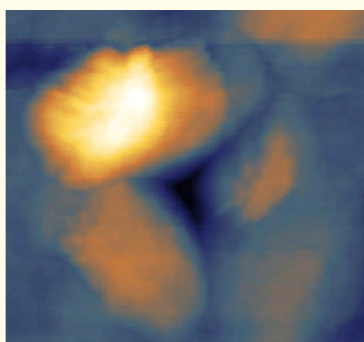


Figure 4: The effect of the nanoindenter on 3Y-TZP-HA nanocomposite coating.

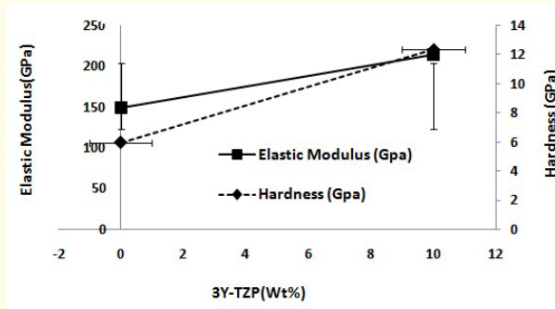


Figure 5: Variation of young's modulus and hardness of nanocomposite coatings versus 3Y-TZP content.

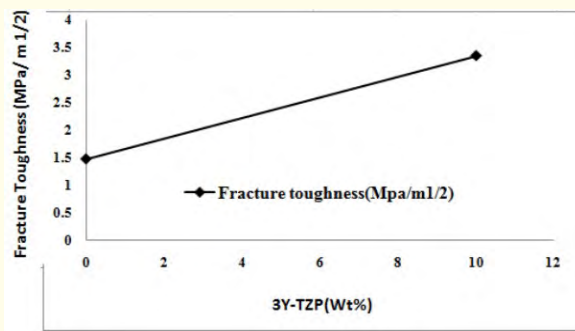


Figure 6: Variation of fracture toughness for nanocomposite coatings versus 3Y-TZP content.

**The dissolution behavior of HA and 3Y-TZP-HA coats**

Figure 7 and Figure 8 show the dissolution behavior of HA and 3Y-TZP-HA coatings with respect to Ca and P ions release in a physiological saline solution (0.9% NaCl) as a function of time. It could be observed that the dissolution rate of 3Y-TZP-HA coat was lower than that of the pure HA coat.

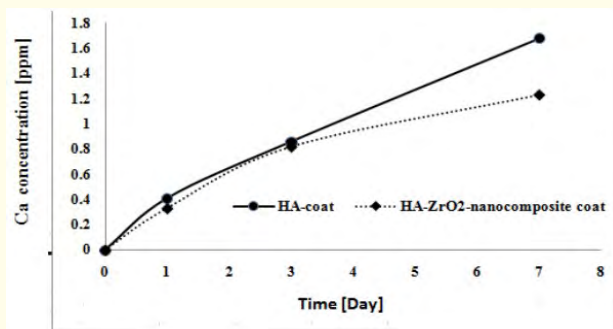
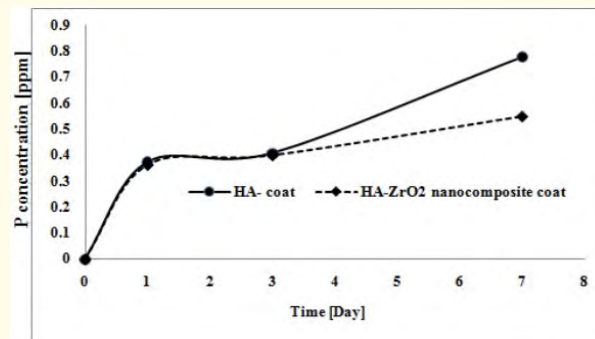


Figure 7: Comparison between the dissolution behavior and ca ion release of HA and 3Y-TZP-HA coatings after heat treatment at 600°C for 1h.



**Figure 8:** Comparison between the dissolution behavior and p ion release of HA and 3Y-TZP-HA coatings after heat treatment at 600°c for 1h.

## Discussion

This study was aimed to fabricate a free-crack 3Y-TZP-HA coating on A-3Y-TZP20 nano-composite substrate using a sol-gel process for endosseous dental implant application. Tetragonal to monoclinic transformation may stem from hydrothermal aging in the wet environment of the oral space. This phenomenon is usually known as the low temperature degradation, by which the energy barrier for tetragonal to monoclinic transformation is reduced. This phenomenon is due to the formation of water components which are not yet fully known within the zirconia network. As a result, tetragonal to monoclinic transformation is gradually spread over the surface, subsequently penetrating into the depth of material. This transformation slowly progresses at the temperature of oral space. The existence of large amounts of monoclinic phase is known to be deleterious to the mechanical properties of zirconia. Moreover, this may damage the long term clinical success of zirconia-based restorations [31]. A coat deposited on zirconia substrate may act as a barrier preventing water penetration into the substrate, providing an enhanced control over the degradation process at the low temperature. Commercially, plasma spraying is the most commonly used technique for coating deposition in dental implants [25] and a few studies have been directed toward using the sol-gel method. Some studies have optimized the spraying parameters for 3Y-TZP deposition to use the plasma spray method [21]. Application of plasma sprayed-HA coating on titanium endosseous dental implant encounters several problems; these are such as changes in the structure and chemical properties of HA coating, the formation of undesirable phases during the deposition process, high thickness and density in homogeneity [13], compositional degradation [22], and the weakening of the coating-metal interfacial strength due to the formation of a thick coating layer [24]. These shortcomings can be overcome by using the sol-gel method for coating deposition because it is known to be a low temperature process providing more homogeneity and high purity. Therefore, the aim of this study was creating a free crack and pit coating on the alumina (20%vol)-3-yttrium stabilized tetragonal zirconia substrate using the sol-gel method. According to investigations by Du., *et al.* [26], the fracture toughness and hardness of HA-ZrO<sub>2</sub> composite coating applied on titanium alloy by laser cladding were measured to be 1.25 MPa.m<sup>1/2</sup> and 340 kg.mm<sup>1/2</sup>, respectively, thereby indicating increased values as compared to those of HA coating. In the present study, the hardness and fracture toughness of the 3Y-TZP-HA coating were found to be greater than those obtained for HA-ZrO<sub>2</sub>, based on the reports by Du., *et al.* [26]. This difference can be attributed to the different coating process, chemical composition and the formation of the nano-structured coating (Figure 3). Also, Vasconcelos and Barrete [16], who studied the mechanical properties of a 3Y-TZP-HA composite developed by the modified sol-gel method, revealed an increase in hardness and fracture toughness as a result of stress-induced phase transformation, as evidenced by SEM observations. Also, the studies conducted on plasma-sprayed ZrO<sub>2</sub>-HA composite coatings have reported higher mechanical properties and lower dissolution rate, in comparison to those of HA coating [20,27]. As stated in the previous section, the increase in the young's modulus and hardness of the 3Y-TZP-HA coating, in comparison to HA coating, is associated with the presence of zirconia nano-particles as well as the formation of nano-structured coating, which is consistent with the data reported by Morks and Akira [21]. Based on the XRD analysis from the previous studies, the apatite phase begins to appear

at 400°C, whereas the complete crystallization requires a subsequent heat treatment at temperatures above 500°C Kim., *et al.* [24]. In practice, HA coats fabricated by the sol–gel method are usually accompanied by several by-products such as tri-calcium phosphate(TCP), tetra calcium phosphate (TTCP), calcium oxide(CaO), and a considerable amount of amorphous phases [28]. In this study, 3Y-TZP-HA and HA coatings heat treated at 900°C and aged for 12 h revealed significant deep cracking, together with some pitting, although cracks in the HA coat were more and deeper (see Figure 2). With increasing the aging time to 18h and decreasing the temperature to 700°C, the number of cracks and pits was reduced in both coatings (Figure 2). However, based on SEM observations, the proper temperature and aging time were found to be 600°C and 24h (Figure 2), which caused the coatings with minimal pits and cracks. It seemed that increasing the aging time to 24h led to the completion of the polymerization process and the effective removal of volatile substances and solvents; therefore, heat treatment at higher temperatures was not required. As for plasma-sprayed HA coatings, due to the rapid temperature fluctuations during solidification, severe cracking was frequently observed and this could be a disadvantage for the plasma-sprayed method [29]. As a result, very low heating and cooling rates were selected in this work to minimize the thermal fluctuations during heat treatment. Although previous studies have reported a high dissolution rate for HA coatings prepared by the sol-gel method in a short time, this can be a serious problem limiting their long-term applications, where the coating layer needs to possess a low desorption rate, a high intrinsic strength and a uniform structure. In this study, the 3Y-TZP-HA nano-composite coating prepared by the sol-gel method revealed a higher strength and a lower dissolution rate, as compared to the HA coating. The XRD pattern of HA coating (see Figure 1) showed the presence of calcium oxide peak; thus, the higher dissolution rate of HA, in comparison to 3Y-TZP-HA, could be due to the calcium oxide phase in the phase composition of HA coating. Stoichiometric HA had the minimum solubility and the highest stability. Based on Lee., *et al.* [30], the single-phase HA coating had the highest amount of free calcium ions, while the kinetics of dissolution for composite coatings was slower. In the case of composite coatings, due to the presence of reinforcing particles, the HA contact area with solution was smaller, resulting in the negligible release of Ca and P ions into the solution during the first day of immersion. The zirconia particles were not dissolved into the solution and remained in the coating, while the HA contact with solution was reduced due to the presence of zirconia particles; hence, the dissolution rate was further decreased. Lee., *et al.* [30] also revealed that the free calcium concentration in the pure HA was greater than that of composite samples and the dissolution was increased with increasing the immersion time. In the present work, the dissolution behavior of 3Y-TZP-HA coating was determined by measuring the dissolved Ca and P ions using ICP method. The dissolution rate of Ca and P ions for the 3Y-TZP-HA coating was lower than that of HA coating. This reduction could be attributed to the chemical composition of the composite coating, which is consistent with the previous studies [24]; also, the higher dissolution rate for HA coating could be related to the presence of calcium oxide in the coating structure, as evidenced by XRD analysis (Figure 1).

## Conclusions

Sol–gel derived 3Y-TZP-HA coats were dip-coated on A-3Y-TZP20 nano-composite substrates. A 3Y-TZP-HA coating was achieved after heat treatment at 600°C and aging for 24h so that no significant evidence showing cracking and pitting was observed. The 3Y-TZP-HA coats dissolved in the physiological saline solution at a slower rate were compared to the HA coats. The 3Y-TZP-HA nano-composite coating revealed superior mechanical properties, as compared to HA coat, in terms of young's modulus, hardness and fracture toughness. Therefore, 3Y-TZP- HA nano-composite coat with minimal cracks and pits can be introduced as a promising way for the control of the low temperature degradation process.

## Acknowledgements

The authors would like to appreciate the Department of Materials Engineering, at Isfahan University of Technology, and School of Dentistry, at Isfahan University of Medical Sciences, for their scientific supports and cooperation.

## Bibliography

1. M Andreiotelli., *et al.* "Are ceramic implants a viable alternative to titanium implants: A systematic Literature review". *John Wiley and sons* 25 (2009): 1-61.



2. M Hobkirk. "Dental implantes: Biomaterial, Biomechanical and biological consideration". *Dental Implants* 7.1 (2008): 27-35.
3. CJ Hochscheidt., *et al.* "Implantes dentarios em zirconia: uma alternativa para o presente ou para o future? (Parte 2)". *Dental Press Implantology* 6 (2010): 114-124.
4. G Manivasagam., *et al.* "Biomedical implantes: Corrosion and its prevention –A review". *Recent Patents on Corrosion Science* 2 (2010): 40-54.
5. H Garg., *et al.* "Implant surface modifications: A review". *Journal of Clinical and Diagnostic Research* 6.2 (2012): 319-324.
6. N Adya., *et al.* "Corrosion in titanium dental implants: literature review". *The Journal of Indian Prosthodontic Society* 5.3 (2005): 126-131.
7. M Cattani-Lorente., *et al.* "Low temperature degradation of a Y-TZP dental ceramic". *Acta Biomaterialia* 7.2 (2011): 858-865.
8. SJ Ferguson., *et al.* "Biomechanical comparison of different surface modifications for dental implants". *International Journal of Oral and Maxillofacial Implants* 23.6 (2008): 1037-1046.
9. M Gahlert., *et al.* "A comparison study of the osseointegration of zirconia and titanium dental implants. A Biomechanical evaluation in the maxilla of pigs". *Clinical Implant Dentistry and Related Research* 12.4 (2010): 297-305.
10. R Gruber., *et al.* "Acid and Alkali etching of grit blasted zirconia: impact on adhesion and osteogenic differentiation of MG63 cells *in vitro*". *Journal of Dental Materials* 31.6 (2012): 1097-1102.
11. G Marques., *et al.* "Bone Healing in Titanium and zirconia implants surface: A pilot study on the rabbit tibia". *Revista Sul-Brasileira de Odontologia* 10.2 (2013): 110-115.
12. A Noro., *et al.* "Influence of surface topography and surface physicochemistry on wettability of zirconia (tetragonal zirconia polycrystal)". *Journal of Biomedical Materials Research Part B Applied Biomaterials* 101.2 (2012): 34- 39.
13. SK Coco. "A mechanical and histological study of functionally graded hydroxiapatite coatings". *The University of Tennessee Health Science Center* (2008): 1-34.
14. KH Lm., *et al.* "Hydroxiapatite/Titania coatings on Titanium by sol-gel process". *Biomaterial Research* 10 (2006): 224-230.
15. AV Sabane. "Surface characteristics of dental implants; A review". *Journal of Indian Academy of Dental Specialist Researchers* 2 (2011): 18-21.
16. HC Vasconcelos and MC Barrete. "Tailoring the microstructure of sol-gel derived Hydroxiapatite/zirconia Nanocrystalline composites". *Nanoscale Research Letters* 6.1 (2011): 20.
17. Z Evis. "Reactions in hydroxylapatite – zirconia composite". *Ceramic International* 33 (2007): 987-991.
18. MH Fathi and A Hanifi. "Sol-gel derived nanostructure hydroxiapatite powder and coating: aging time optimization". *Advances in Applied Ceramics* 108.6 (2009): 363-368.
19. D Tang., *et al.* "Evaluation of mechanical reliability of zirconia –toughened Alumina composites for dental implants". *Ceramic International* 38.3 (2011): 2429-2436.
20. GR Anstis., *et al.* "A critical evaluation of indentation techniques for measuring fracture toughness: 1. Direct crack measurements". *Journal of the American Ceramic Society* 64.9 (1981): 533-538.
21. MF Morks and K Akira. "Microstructure and mechanical properties of HA/ZrO<sub>2</sub> coatings by gas tunnel plasma spraying". *Joining and Welding Research Institute* 36.1 (2007): 47-51.

22. F Lei., *et al.* "The evaluation of powder processing on microstructure and mechanical properties of hydroxiapatite / Yttria stabilized zirconia (YSZ) composite coatings". *Journal of Surface and Coatings Technology* 140 (2001): 263-268.
23. WC Oliver and GM Pharr. "Measurement of hardness and elastic modulus by instrumented indentation: Advances in understanding and refinements to methodology". *Journal of Materials Research* 19.1 (2004): 1-20.
24. HV Kim., *et al.* "Sol-gel derived fluor-hydroxiapatite biocoatings on zirconia substrate". *Biomaterials* 25.15 (2004): 2919-2926.
25. K Cheng., *et al.* "The effect of triethanolamine on the formation of sol–gel derived fluoroapatite/hydroxyapatite solid solution". *Materials Chemistry and Physics* 78.3 (2003): 767-771.
26. HY Du., *et al.* "Influence of zirconia on hydroxiapatite coatings on Ti-alloy by Laser Cladding". *Transactions of Tianjin University* 9 (2003): 292-295.
27. T Kokubo and H Takadama. "How useful is SBF in predicting in vivo bone bioactivity". *Biomaterials* 27.15 (2006): 2907-2915.
28. A Wennerberg and T Albrektsson. "On implant surfaces; A review of the current knowledge and opinions". *International Journal of Oral and Maxillofacial Implants* 25.1 (2010): 63-74.
29. I Demnati., *et al.* "Plasma sprayed apatite coatings: review of physical –chemical aspects and their biological consequences". *Journal of Medical and Biological Engineering* 17 (2013): 43-49.
30. EJ Lee., *et al.* "Fluoridated apatite coatings on titanium obtained by electron-beam deposition". *Biomaterial* 26.18 (2005): 3843-3851.
31. V Lughì and V Sergo. "Low temperature degradation –aging of zirconia: A critical review of the relevant aspects in dentistry". *Dental Materials Journal* 26.8 (2010): 807-820.

**Volume 6 Issue 6 December 2016**

**© All rights reserved by Moluk Aivazi., *et al.***